

Coverage bias in the HadCRUT4 temperature series and its impact on recent temperature trends.

UPDATE

Hybrid temperature reconstruction by domain

Kevin Cowtan, Robert G. Way

February 5th, 2014

1 Hybrid temperature reconstruction by domain

This update document describes new versions of the hybrid temperature reconstructions introduced in Cowtan and Way (2014) (henceforth CW14), and builds upon a previous [update of 06/01/2014](#) on the use of separate land and ocean reconstructions.

Different source datasets are evaluated for both for the land surface air temperature observations, and for the global proxy data used in the hybrid calculation to complete the coverage. The impact of the choice of data source on temperature trends over the 16 year period from 1997/01 to 2012/12 is examined. While one of the purposes of CW14 was to highlight the danger of drawing conclusions about global climate change from such short term trends, the period is nevertheless of considerable interest in the development and evaluation of global mean surface temperature calculations. Rapid and localised warming in regions of sparse observations represents a [pathological](#) test case, and the detailed comparison of results across different calculations and data sources may provide useful insights in improving the algorithms.

2 Source data

2.1 In situ temperature data

2.1.1 HadSST3 ocean data

The HadSST3 data from the Hadley centre is a gridded dataset of sea surface temperatures from 1850 to the present (Kennedy *et al.*, 2011). The gridded data are not interpolated or infilled. The observational data are corrected according

to estimates of bias for the given observational platform, including corrections for bucket observations and engine room intake sensors, which may vary from ship to ship.

2.1.2 CRUTEM4 land data

The CRUTEM data provide the land temperatures for use in the HadCRUT temperature data. Both station records and gridded data are available. A recent update (Jones *et al.*, 2012) introduced many additional station records chosen to address coverage issues in poorly sampled regions bringing land coverage to an average of 70% over the study period. As a result the high latitude coverage is good given the limitations of the observational network. Homogenisation of the station records is primarily conducted by the record providers on the basis of their records of changes in the station location or instrumentation. HadCRUT4 reprocesses the CRUTEM4 data by the introduction of terms to represent the uncertainty in homogenisation, exposure and urban heat island corrections, resulting in an ensemble of 100 land temperature realisations. CRUTEM4 coverage and trends for the 16 year study period are shown in Figure (U1a).

2.1.3 GHCN land data

The Global Historical Climatology Network-Monthly (GHCNM, version 3) provide both station records and gridded temperature data in a form suitable for use in place of the CRUTEM4 data (Lawrimore *et al.*, 2011). The coverage of the *gridded* data is rather more limited than CRUTEM4, averaging 50% land coverage over the study period, with fewer Arctic stations especially in Canada and Siberia. However there are many additional stations which are present in the GHCN station data but not in the gridded product. The GHCN station data has been automatically homogenized with a pairwise comparison algorithm (Williams *et al.*, 2012). GHCN coverage and trends for the 16 year study period are shown in Figure (U1b).

2.1.4 BEST land data

The Berkeley Earth Surface Temperature dataset (BEST) provide a new version of the land temperature record using a greatly expanded list of weather stations, automated station homogenisation and infilling of unobserved regions. Infilled gridded data are provided. To obtain a globally complete record, the BEST data would need to be further extrapolated over sea ice and then blended with the extrapolated SST data, however extrapolation from a smoothed dataset is inadvisable and could lead to artifacts. The land temperatures over Antarctica and the blended data at lower latitudes may however be used for comparison with the other datasets.

2.2 Proxy data for hybrid reconstruction

2.2.1 UAH satellite data

The University of Alabama in Huntsville (UAH) lower troposphere (TLT) data (Christy *et al.*, 2007) were investigated in CW14 and found to provide a useful predictor of land surface air temperature on the basis of the kriging statistics of the difference data, cross validation tests (both globally averaged and local) and skill in reconstructing reanalysis data. UAH trends for the 16 year study period are shown in Figure (U2a).

2.2.2 MERRA reanalysis data

The MERRA reanalysis data (Rienecker *et al.*, 2011) is derived from a weather model which assimilates observations from satellites, ships and buoys, radiosondes, and barometers on land. Since land-based temperature readings are missing from this list the data may be used as a predictor of land surface air temperature. Lindsay *et al.* (2014) report that MERRA outperforms other reanalysis products in the Arctic and Screen and Simmonds (2012) report similar results for the Antarctic. However the assimilation of additional data sources (such as the NASA AIRS data from 2002) can cause inhomogeneities in reanalysis records (Sturaro, 2003). MERRA trends for the 16 year study period are shown in Figure (U2b).

3 Temperature reconstruction

Global reconstructions of both the land and ocean data are prepared according to the methods described in the following sections. The reconstructed land and ocean temperature fields are then blended according to the fraction of land plus sea ice in each cell. The ice mask varies from month to month but is held constant from year to year to avoid a potential bias due to the transformation of cells from ice to open ocean. Sea ice coverage is determined from the HadISST data using the *minimum* of the sea ice concentration on the period 1981-2010 for each cell and each month. This is a change from the long reconstruction described in the [update of 06/01/2014](#) in which the *median* of the sea ice concentration was used on the grounds that the minimum ice mask is more representative over recent years. Note that the resulting ice mask gives a lower ice cover than in any individual month in the reference period because the sum of the minimums for each cell is lower than the minimum of the sum over all cells.

HadCRUT4 places a lower bound of 25% on the land content of a cell so that air temperature observations from small islands can influence the surrounding ocean cell: this step is not used in the reconstructions described here.

3.1 Sea surface temperature reconstruction

Sea surface temperatures (SSTs) are reconstructed by kriging for all of the temperature reconstructions. While CW14 found a weak correlation between the SSTs and the satellite data, the benefit of applying the hybrid calculation is marginal especially at high latitudes where unobserved cells are most likely to occur, so the simpler kriging calculation is used. The e-folding range of the covariance function is a little over 900km - Table (U1).

3.2 Land temperature reconstructions

Three land reconstructions were produced for each source dataset, by kriging, hybrid with the UAH data and hybrid with the MERRA data. In the case of kriging, the e-folding range of the covariance function (which controls how far temperatures may be extrapolated) is about 750km for the CRUTEM4 data (Table U1). The range for the GHCNv3 data is somewhat longer; the reasons for this difference are unclear.

3.2.1 UAH

The UAH data are used as a surface temperature proxy using a scale factor $s = 1$, in accordance with CW14. Tests with middle troposphere data from both UAH and STAR (Zou, 2013) produced less benefit when compared to the UAH TLT data.

The e-folding range of the covariance function drops by about 200km in comparison to kriging. The reduction in range arises from the fact that some of slowly varying temperature signal has been subtracted from the data (CW14 equation 1), and as a result the remaining noise plays a greater role in shaping the variogram.

3.2.2 MERRA

The kriging range for the MERRA hybrid calculation much lower than for the other cases. This arises from the fact that the MERRA data is a good predictor where observations are present, i.e. the differencing step takes out most of the temperature signal from the data. As a result most of the reconstructive power is handed over from interpolation from existing stations to infilling using the MERRA data. The MERRA reconstruction is therefore somewhat independent of the other methods, and in consequence gives somewhat different results.

4 Analysis

Temperature trends covering the period 1997/1 to 2012/12 are given in Table (U2) for kriging, hybrid with UAH and hybrid with MERRA reconstructions based on both the HadCRUT4 land ensemble and the GHCN gridded land data.

Trends are given for the whole planet and for three latitude bands covering the Arctic, lower latitudes and Antarctic. Global temperature series for all 6 reconstructions are also shown in Figure (U3).

The HadCRUT4 kriging and MERRA hybrid reconstructions give similar global trends. The MERRA hybrid gives higher trends in the Arctic and at lower latitudes. However it shows no trend over Antarctica, as a result of a cooling trend over the Antarctic sea ice which is absent from the other reconstructions, as well as lower trends over the Antarctic continent. The UAH hybrid shows a greater trend in Antarctica (which is the most sparsely sampled region of the planet) but is otherwise similar to the kriging reconstruction.

The GHCN reconstructions show a lower global trend, primarily due to a reduced trend in the Arctic. This arises in part from the sparsity of Arctic stations in the GHCN data, and can be reproduced in the HadCRUT4 data by reducing coverage to match the GHCN data. The hybrid reconstructions mitigate this lack of coverage, with the UAH hybrid showing the greatest trend. However there are also differences in the temperature data arising from the additional GHCN homogenisations; these will be discussed in a future update.

The BEST data for the study period support a warming trend over the Antarctic continent (in contrast to the MERRA hybrid). As already noted this data may not be extended over sea ice due to the problem of extrapolation from smoothed data. However the BEST data suggest a lower trend of $0.03^{\circ}\text{C}/\text{decade}$ in the low/mid latitude band - if this is correct it would lead to a downward adjustment of around $0.01^{\circ}\text{C}/\text{decade}$ in the results presented here and in CW14.

The map series for the three HadCRUT4 based reconstructions are shown in Figure (U4). The similarity between the kriging and UAH hybrid reconstructions is clear, however the faster Antarctic warming in the UAH hybrid is also apparent.

As previously noted the MERRA reconstruction differs somewhat in that the e-folding range of the kriging covariance function is substantially reduced. The effect of the e-folding range can be seen by comparing the trend maps for the 3 reconstructions, particularly in Antarctica. The kriging reconstruction is smoothest and determined solely by the station values. The UAH reconstruction shows some features not in the kriging reconstruction. The MERRA reconstruction shows many localised features, and the stations only influence a rather limited region around them. The MERRA hybrid also produces very rapid warming in the unobserved region in southern Africa, which is rejected by all of the other temperature reconstructions.

A potential weakness of the MERRA reconstruction is that the barometer and radiosonde observations tend to be concentrated in the same regions as the *in situ* temperature observations. If the radiosonde data play a dominant role in determining surface temperature in the model then it is possible that the skill of the MERRA data in the observed regions does not transfer to skill in reconstructing unobserved regions. Comparison of Figures (U2b) and (U4a,b) suggests that the MERRA trends for Africa and South America require further investigation (however these appear to arise from trends over the whole study period rather than discontinuities associated with the introduction of new data

sources). For this reason the UAH hybrid is currently favoured, although the results obtained using the MERRA data as a proxy provide an interesting insight into the behaviour of the hybrid calculation.

References

- Christy JR, Norris WB, Spencer RW, Hnilo JJ. 2007. Tropospheric temperature change since 1979 from tropical radiosonde and satellite measurements. *J. Geophys. Res.* **112**(D6): D06 102.
- Cowtan K, Way RG. 2014. Coverage bias in the hadcrut4 temperature series and its impact on recent temperature trends. *Quarterly Journal of the Royal Meteorological Society* .
- Jones P, Lister D, Osborn T, Harpham C, Salmon M, Morice C. 2012. Hemispheric and large-scale land-surface air temperature variations: An extensive revision and an update to 2010. *J. Geophys. Res.* **117**(D5).
- Kennedy J, Rayner N, Smith R, Parker D, Saunby M. 2011. Reassessing biases and other uncertainties in sea surface temperature observations measured in situ since 1850: 2. biases and homogenization. *J. Geophys. Res.* **116**(D14): D14 104.
- Lawrimore JH, Menne MJ, Gleason BE, Williams CN, Wuertz DB, Vose RS, Rennie J. 2011. An overview of the global historical climatology network monthly mean temperature data set, version 3. *Journal of Geophysical Research* **116**(D19): D19 121.
- Lindsay R, Wensnahan M, Schweiger A, Zhang J. 2014. Evaluation of seven different atmospheric reanalysis products in the arctic. *Journal of Climate* **in press**(2014).
- Rienecker MM, Suarez MJ, Gelaro R, Todling R, Bacmeister J, Liu E, Bosilovich MG, Schubert SD, Takacs L, Kim GK, Bloom S, Chen J, Collins D, Conaty A, da Silva A, Gu W, Joiner J, Koster RD, Lucchesi R, Molod A, Owens T, Pawson S, Pegion P, Redder CR, Reichle R, Robertson FR, Ruddick AG, Sienkiewicz M, Woollen J. 2011. Merra: Nasa's modern-era retrospective analysis for research and applications. *Journal of Climate* **24**(14): 3624–3648.
- Screen JA, Simmonds I. 2012. Half-century air temperature change above antarctica: Observed trends and spatial reconstructions. *Journal of Geophysical Research: Atmospheres (1984–2012)* **117**(D16).
- Sturaro G. 2003. A closer look at the climatological discontinuities present in the ncep/ncar reanalysis temperature due to the introduction of satellite data. *Climate dynamics* **21**(3-4): 309–316.

- Williams CN, Menne MJ, Thorne PW. 2012. Benchmarking the performance of pairwise homogenization of surface temperatures in the united states. *J. Geophys. Res.* **117**(D5): D05 116.
- Zou CZ. 2013. Atmospheric temperature climate data records from satellite microwave sounders. In: *Satellite-based Applications on Climate Change*, Qu J, Powell A, Sivakumar M (eds), Springer Netherlands, ISBN 978-94-007-5871-1, pp. 107–125, URL http://dx.doi.org/10.1007/978-94-007-5872-8_8.

Table U1: Range (i.e. e-folding distance) in km of the covariance function used in the kriging step of the infilling or hybrid calculation for different data and methods.

Data/method	Kriging range (km)
HadSST3 krig	917
CRUTEM4 krig	753
CRUTEM4 UAH	556
CRUTEM4 MERRA	339
GHCNMv3 krig	915
GHCNMv3 UAH	714
GHCNMv3 MERRA	442

Table U2: Temperature trends over the 16 year period 1997/1-2 012/12 in $^{\circ}\text{C}$ decade $^{-1}$ for the whole planet and three latitude bands. The 60S-60N latitude band covers 86.6% of the planet; the other two bands cover 6.7% each.

Data/method	Trend ($^{\circ}\text{C}$ decade $^{-1}$)			
	Global	60N-90N	60S-60N	90S-60S
CRUTEM4 krig	0.114	0.951	0.040	0.239
CRUTEM4 UAH	0.124	0.958	0.042	0.351
CRUTEM4 MERRA	0.112	0.994	0.051	0.013
GHCNMv3 krig	0.092	0.705	0.043	0.124
GHCNMv3 UAH	0.107	0.757	0.046	0.244
GHCNMv3 MERRA	0.099	0.825	0.051	0.001

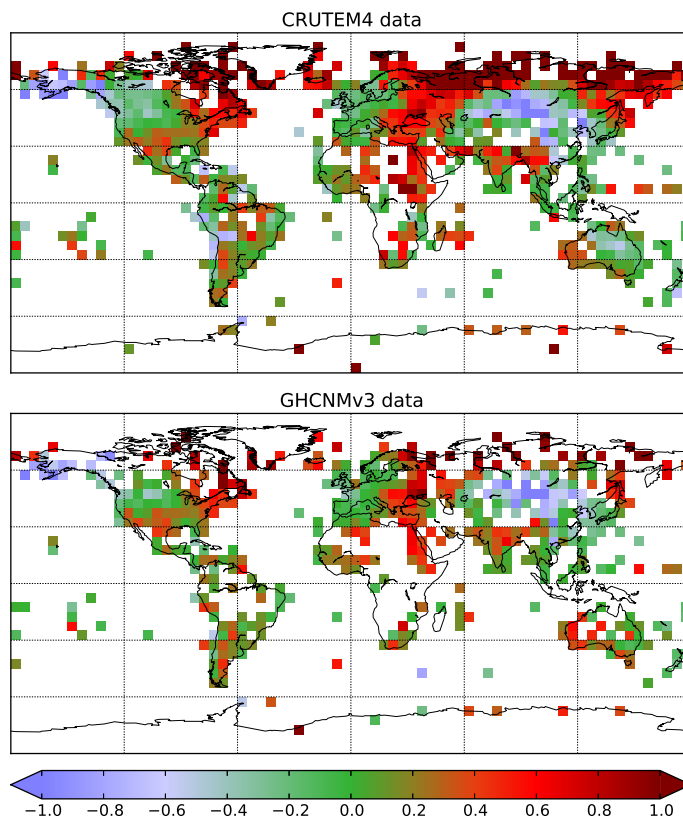


Figure U1: Temperature trends on the 16 year period 1997/01-2012/12 for the source datasets.

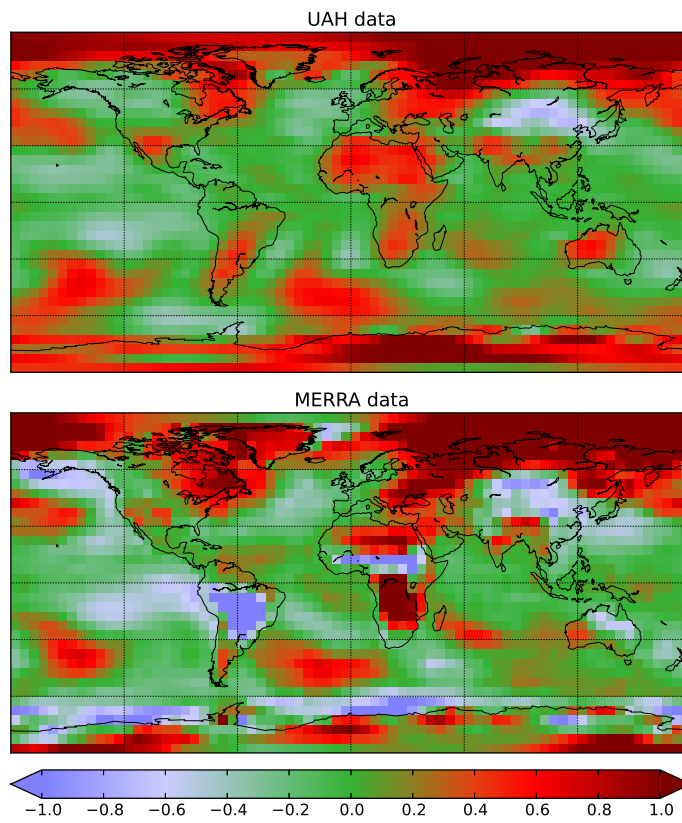


Figure U2: Temperature trends on the 16 year period 1997/01-2012/12 for the proxy datasets.

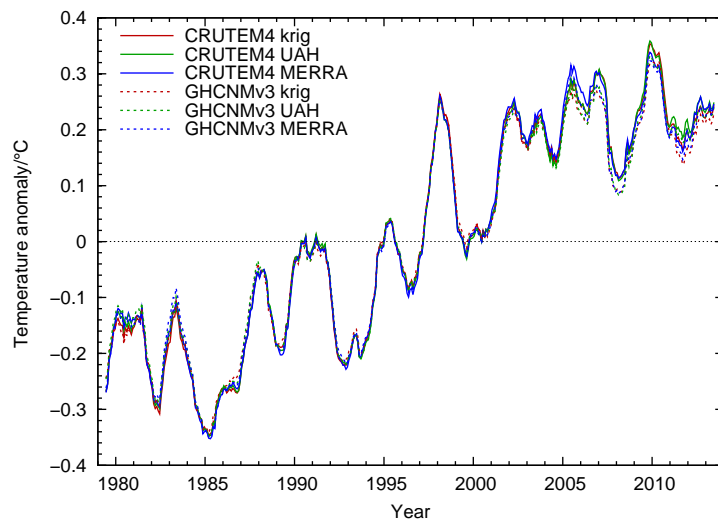


Figure U3: Temperature series for kriging, and UAH hybrid and MERRA hybrid reconstructions starting from the CRUTEM3 and GHCNMv3 *in situ* data.

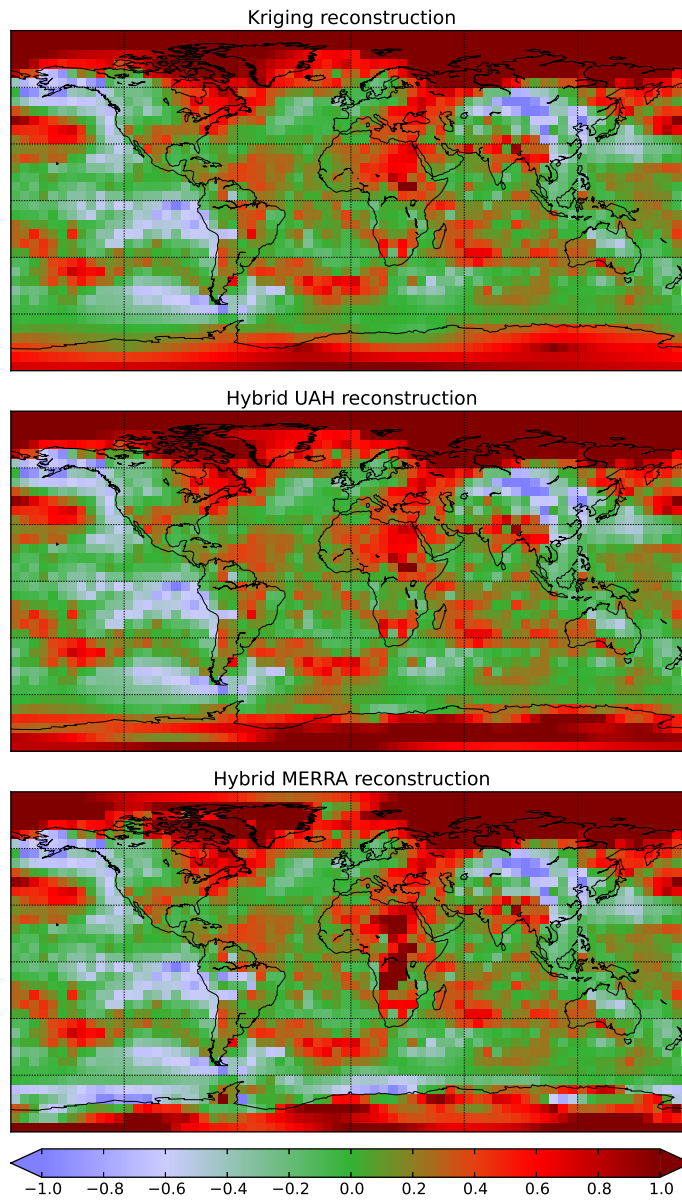


Figure U4: Temperature trends on the 16 year period 1997/01-2012/12 for kriging, and UAH hybrid and GHCN hybrid reconstructions starting from the CRUTEM4 *in situ* data.